Salt movement and its implications on vertical-axis rotation in the Potwar Plateau, northern Pakistan.

By Jorik Poessé

Supervised by:

Prof. dr. W. Krijgsman
Prof. dr. C.G. Langereis
Prof. dr. N. Kaymakcı

Abstract

The Potwar Plateau is formed as a result of the Cenozoic India-Eurasia collision. The deformation front of the Himalayas reached the plateau in Neogene time, where the precambrian evaporite décollement provided a frictionless surface for the most recently created thrust, *The Salt Range Thrust*. The Plateau is filled with a thick molasse of Lower Miocene to Pleistocene age of the Siwalik Group known for its continuous deposition. Only the Holocene appears undeformed, indicating the continuity of the Siwaliks provide an excellent record for the mechanics of the region. In the last 10 million years, the Salt Range as well as the Potwar Plateau plateau exhibited larger-scale movements which are different from the 0-2° CW (clockwise) rotation of the Indian plate (Torsvik et al., 2012) in the past 10 million years. New and existing paleomagnetic data shows a coherent rotational pattern throughout the Potwar Plateau, with no rotation in the Western Plateau and up to 30° CCW rotation in the Eastern Plateau. The differential rotation is explained by the evaporite décollement, being present in the Western plateau resulting in a low-friction environment, forming the the dextral *Kalabagh Fault*, a lateral ramp on the Western margin. The Eastern part of the plateau is marked by 50°/230° trending strikes of fold axes and fault planes. The rotational difference together with the local structures are part of an orocline within the plateau, indicating a deformation phase after deposition and formation of the local structures. A magnetostratigraphic analysis on the Soan Formation of the Siwaliks dated the base of the formation at 3.7 Ma with the top at approximately 2.2 Ma, which was concluded to be the oldest possible age for the most recent deformation phase. This is assumed to be in the same timeframe as the onset of ramping of the Salt Range Thrust. Due to the influence of the evaporite décollement on the larger part of the area, it is suggested that the Potwar Plateau and the Salt Range are a local expression of the India-Eurasia convergence heavily influenced by salt tectonics.

Introduction

Pakistan is for the larger part situated on the Indian plate where the geology in the Northern regions is mostly affected by the Cenozoic India-Eurasia collision. The two plates have converged up to 3600 ± 35 km since 52 Ma (Van Hinsbergen et al., 2012). In Northern Pakistan, this resulted in a series of thrusts younging from North to South. Remnants of the Eurasian plate can be found in Kohistan and the far North of Pakistan, in the hanging wall of the MMT (Main Mantle Thrust). The Kohistan complex was placed onto the Indian Crust, bringing up mantle rocks and metamorphic facies. It is bounded by the Main Karakorum Thrust to the north and the MMT to the south. Faulting in the Himalayan front has progressively moved southward (Powell and Conaghan, 1973; Yeats and Lillie, 1991), resulting in the stacking of the Indian continental plate internally (Gansser, 1981; Yeats and Lillie, 1991). The Lesser Himalayas, with the MMT to the north and the MBT (Main Boundary Trust) to the south, are characterised by intense deformation, exposing Precambrian basement up to Paleocene sediments. South of the MBT is the Potwar Plateau, known for the Precambrian evaporite used as décollement for the last Himalayan thrust exposed at the surface (Fig. 1). The décollement has been thrusted up, creating a mountain range in the process, the *Salt Range* at the southern boundary of the plateau. The front of the collision reached and affected the Potwar plateau in Neogene time. Although older faults are present in the basement, most structures are developed solely due to the India-Eurasia collision. The Eastern side of the Plateau is bounded by the Koth thrust, a major tectonic boundary where the regime is extremely different from that in the Potwar Plateau (Klootwijk et al., 1986). The Western side is bounded by the Kalabagh Fault, a dextral fault cutting through the Salt Range formations with an apparent offset of approximately 80km. A structure named the *Mianwali Re-entrant* marks the western side of the fault.

The Potwar Plateau has deposits ranging from a Precambrian basement up to Pleistocene molasse sediments. It was raised north of the Salt Range and is mostly filled by Miocene to Pliocene sediments of the Siwalik group, a thick molasse found in the Potwar plateau due to the creation of a continuous deposition centre caused by the uplift and erosion of the Himalayas. The evaporites of Precambrian age have been recently activated, making the Salt Range an area of active salt tectonics (Yeats et al., 1984). The Salt Range as well as the Potwar Plateau plateau exhibit larger-scale movements which are significantly different from the 0-2° CW (clockwise) rotation of the Indian plate (Torsvik et al., 2012) in the past 10 million years.

Sedimentation rates of the Siwaliks in the Potwar Plateau have gradually increased from 12 to 30 cm/kyr until at least 7.9 Ma (Johnson et al., 1985), matching the approximate earliest age of

deformation and thrust-related structures. This is shown in the record as a hiatus in the Northern, more deformed part of the Potwar Plateau. Late-orogenic sedimentation is suggested to have resumed 2.7 Myr ago, at 2.1 Ma creating the Soan Syncline, an asymmetrically folded syncline in the North of the Potwar Plateau. The Salt Range ramping event was estimated to initiate 2.2 Myr ago, continuing passively until today (Johnson et al., 1986).

Seismic reflection studies have shown a detachment of the evaporite layer and the crystalline basement (Lillie et al., 1985), attributing to a historically low seismic activity in the area (Yeats et al., 1984). Due to this recent ramping, Siwalik strata as young as 0.4 Ma can be strongly deformed in the South of the Potwar Plateau. This information and the fact that only the Holocene alluvium appears undeformed (Yeats et al., 1984) indicates the continuity of the Siwaliks provide an excellent record for the mechanics of the region.

Siwalik sediments from the Pleistocene were were first dated using magnetostratigraphy in the Pabbi Hills in the East of the Potwar Plateau (Keller et al., 1977), which highlighted a change of Siwalik to alluvium deposition when the primary source changed from the Himalayan orogeny to a more local sedimentary terrane. They were later dated in the Eastern Salt Range (Opdyke et al., 1979). For part of the Middle Siwaliks the same was done near the village of Dhok Pathan (Barndt et al., 1978). A biostratigraphy was published around the same time (Pilbeam et al., 1977). This led

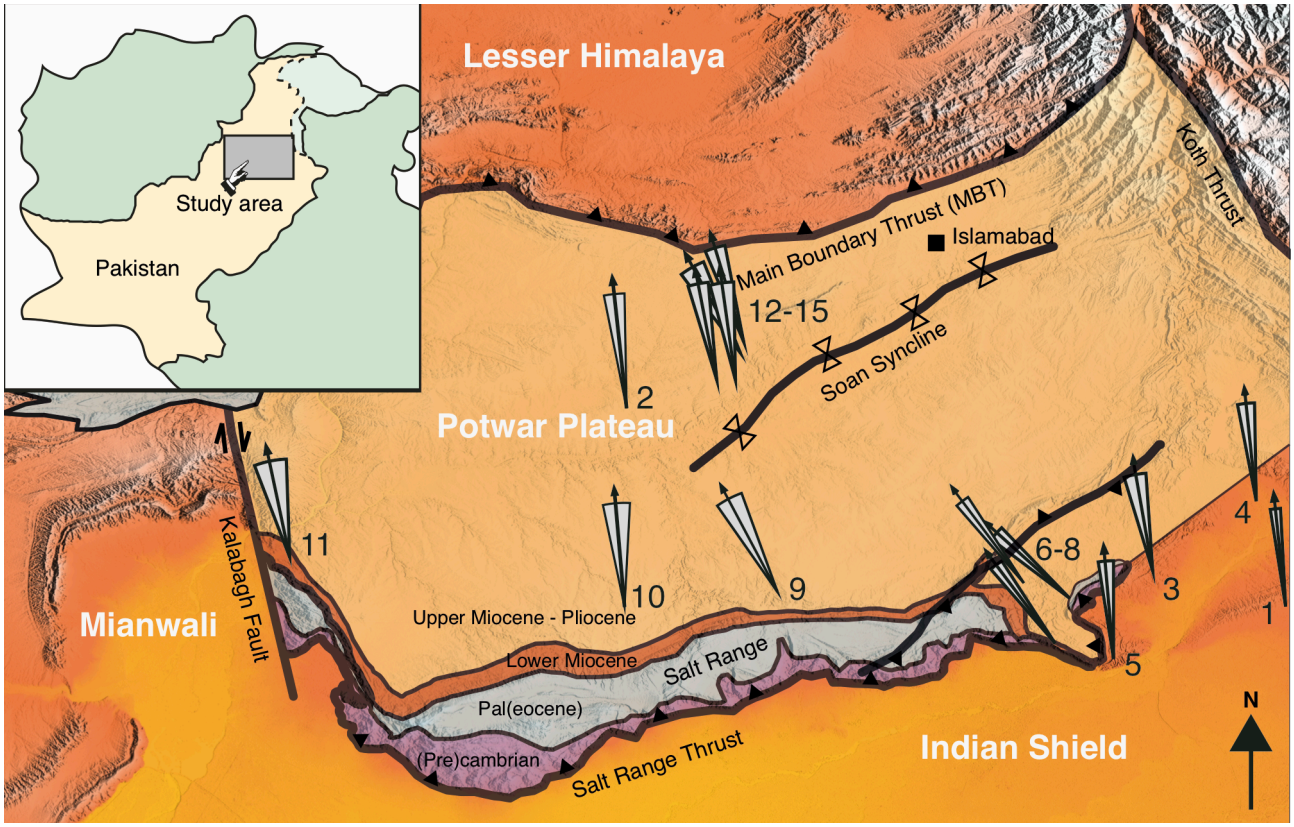

Figure 1 Published tectonic rotations in the Potwar Plateau. From Keller et al., 1977: Pabbi Hills (1); from Barndt et al., 1978: Dhok Pathan (2); from Opdyke et al., 1979: Mangla Samwal (3), Rohtas (4) and Chambal Ridge (5); from Opdyke et al., 1982: Kotal Kund (6), Dhala Nala (7), Tatrot (8), Chakwal Baun (9), Nagri (10) and Dhaud Kel (11); From Tauxe & Opdyke et al., 1982: Kaulial Kas (12), Malawalla Kas (13), Bora Kas (14) and Rhata Kas (15).

to a magnetostratigraphic framework, correlated to mammalian taxes, published in a series of papers (Barry et al., 1982; Johnson et al., 1982; Opdyke et al., 1982; Tauxe and Opdyke, 1982). Part of the Miocene-Pliocene was later included (Johnson et al., 1985).

The deformation can be partly seen in regional tectonic rotations. Magnetostratigraphic columns provided vertical-axis rotations (e.g. Barndt et al., 1978; Tauxe and Opdyke, 1982), but do not give definitive movements of the plateau itself. Rotations of 0-20° CCW were found in Upper Miocene sediments, from 0-20° CCW (counter-clockwise) in the North to 30-40° CCW in the Salt Range (Figure 1). Also it must be noted that tectonic rotations in the Salt Range area are possibly influenced by salt-related faulting, where the interior of the Plateau is less affected. The extensive sedimentary and paleomagnetic dating record do not provide a solution for the significant mechanical changes throughout the Potwar Plateau. This includes the extent of the evaporite substrate which is still under debate. Here, we present a new study on the Upper Miocene and Pleistocene sediments in the Potwar Plateau is done to provide constraints on the age and kinematics of the region

The geological record indicates the absence of evaporites underlying the North of the plateau. To assess the mechanics and its relation to the evaporite substrate of the Potwar Plateau, a more distributed data set is necessary in addition to currently available data. New data was collected with the aim to acquire more information about stable parts of the basin. It is combined with previously acquired data to further explain the kinematics of the Potwar Plateau and its relation to the salt mechanics and thrusting in the region. To date the onset of late-orogenic sedimentation a magnetostratigraphic data set was also acquired in the North of the Potwar Plateau where an angular unconformity marks the onset of sedimentation in Upper Miocene to Pliocene times.

Paleomagnetic data from the two areas are used to investigate the vertical-axis rotation of the Upper Miocene part of the Siwaliks and the onset of sedimentation of the Pleistocene-Pliocene sediments and its relation to the salt movement, which is assumed to have initiated between 2 and 5 Myrs ago. The Upper Miocene is therefore expected to be affected by the salt movement, showing a CCW rotation as observed in the literature.

Correlation to the known magnetostratigraphic column will provide the timeframe of re-sedimentation and therefore the angular unconformity. Kinematic analysis on the Upper Miocene - Pliocene sediments will determine the rotational setting of the Potwar Plateau.

Stratigraphy of the Potwar Plateau

Late precambrian evaporites unconformably overly a crystalline basement of the Indian shield, exposed in the foreland bulge about 80km south of the Salt Range (Khan et al., 1986; Grelaud et al., 2002). The evaporites are the *Salt Range formation* and form the main décollement level of the region. It can be found exposed in the Western Salt Range, but it is either depleted or not exposed in the East. (Gee and Gee, 1989). Cambrian deposits are present throughout the Salt Range, and have been observed in wells. These deposits are named the *Jhelum* group and are solely of marine origin (Khan et al., 1986) with a few observations of igneous rocks of the Khewra traps which intruded into the evaporite layer (Warwick, 1993). The Lower and middle Cambrian, directly above the Salt, is mostly sandstones with some shales and Salt pseudomorph beds (Wensink, 1972). The present thickness ranges from 500 to 1000m, depending on deformation processes (Grelaud et al., 2002) and are gradually thinning from east to west. (Khan et al., 1986). Although there are some indications of Silurian, Devonian and Carboniferous deposits (Wensink, 1972; Warwick, 1993), most of the region is characterised by a large hiatus from the Cambrian up to the Permian.

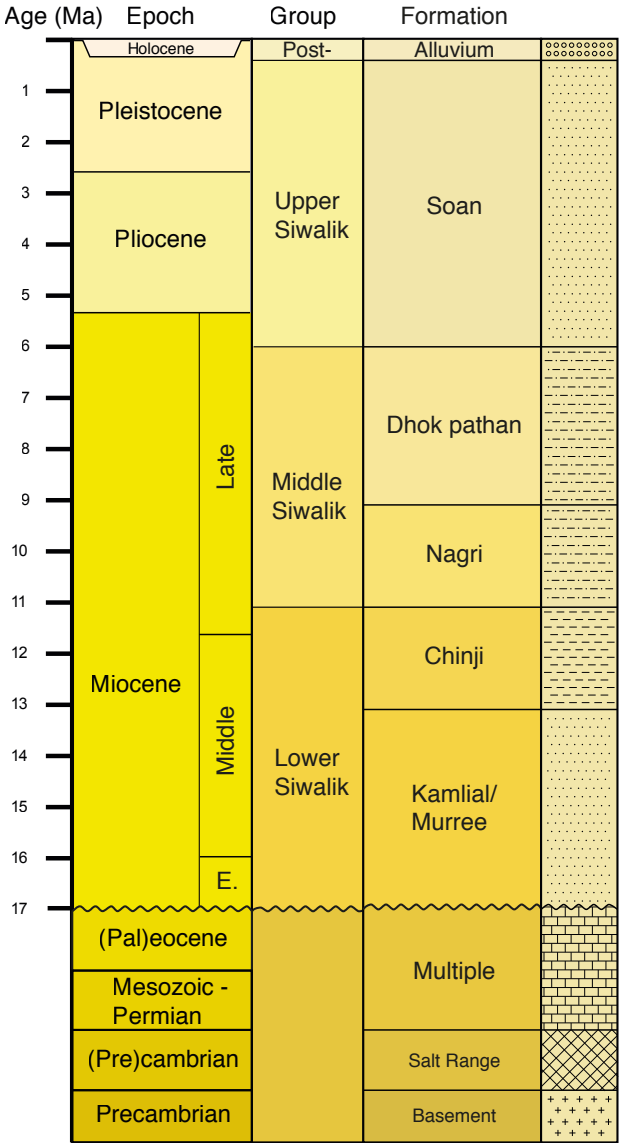

Figure 2 Stratigraphy of the Potwar Plateau with simplified pre-Siwalik formations. Altered from Gee and Gee 1989 and Grelaud et al., 2002.

The Permian directly overlies the Precambrian evaporites in the West. The *Nilawahan* group starts with glacial deposits into dominantly marine deposits with some fluvial sandstones (Khan et al., 1986). Permian to Cretaceous rocks are main ingredients for the petroleum systems found in the Potwar Plateau, but are not present throughout the whole region. The Permian and Cretaceous is more prevalent in the west whereas Jurassic is more present in the east. Paleocene and Eocene

shallow marine foraminiferal limestones mostly overlie the Permian in the Eastern Salt Range. Eocene limestones are the hard tops of the Salt Range and mark the complete withdrawal of the sea (Khan et al., 1986). This is evident from the Oligocene which is a time of uplift and erosion noted in the absence of sediments in the area (Grelaud et al., 2002). Only fluvial sediments of Miocene age follow, creating a large hiatus in the stratigraphy.

The uplift and erosion of the Himalayas in the last 15 Myr has led to the deposit of the well-known molasses of the Siwalik Group, into the foreland basin. Recent Siwalik deposits are from an environment similar to the recent fluvial conditions. In parts of Pakistan and India, a near continuous record has been preserved from 17 to 1 Ma (Stanley, 2005). The Siwaliks are subdivided into Lower, Middle and Upper Groups, where the first two are of Miocene age and the latter continues into the Pliocene-Pleistocene, although the most recent deposits may be referred to as *Post-Siwaliks* (e.g. Johnson et al., 1982; Yeats et al., 1984). The Lower Siwaliks consist of the *Kamlial, Murree* and *Chinji* formations. The first two are mostly basal sand bends, sometimes referred to als the *Rawalpindi Group*, in contrast with the more silty redbed of the *Chinji*. The Middle Siwaliks in the Potwar Plateau are a change from the sandy *Nagri* formation going into the brown silts of the *Dhok Pathan* formation, which can have a total thickness up to 800m thick in the Potwar Plateau (Johnson et al., 1985). The formations of the Lower and Middle Siwalik have been dated (compiled in Johnson et al., 1985), and correlated to the most recent geological time scale by Ogg et al., 2016 (Figure 2). The Upper Siwalik comprises only the *Soan* formation, of which the base is not clearly defined. Its deposition can be associated with the the resumption of sedimentation in the late-orogenic stadium of faulting, or onset of ramping of the Salt Range (Johnson et al., 1986).

Geological structure

Several north-dipping normal faults are present throughout the Precambrian basement and the Eocambrian evaporites due to rifting at that time. There is a large hiatus, even more so tectonically than stratigraphically, from Cambrian through the Jurassic break-up of Gondwana, until onset of collision between the Indian and Eurasian plate. Eocene limestones are the last marine deposition, indicating the onset of the India-Eurasian collision.

The Kamlial formation is the only Siwalik formation preserved in the footwall in the MBT and it is therefore suggested that thrusting along this boundary occurred at the latest in the Lower Miocene (Grelaud et al., 2002). South of the MBT is the North-Potwar Deformed Zone, suggested to be a set of imbricated sheets forming a passive roof duplex with a roof thrust at the base of the Lower Miocene (Jaswal et al., 1997). The Chinji formation is first deposited in the South Potwar Basin as well as in the footwall of the Salt Range — but the youngest Chinji sediments are cut off by the Salt Range thrust, suggesting thrusting events have happened after deposition, placing it in the late

Miocene. Syn-tectonic deposition of the Middle Siwaliks (Nagri and Dhok Pathan formation) in the footwall further confirm this. It has been suggested that at 10 Ma the orogenic system in the North-Potwar Deformed Zone encountered the evaporite substrate and rapidly moved deformation southward (Grelaud et al., 2002). To the south the *Kalabagh Fault*, a dextral fault, cuts through upper Miocene deposits equivalent of the Soan Formation, suggesting an origin between at latest 5.7 Ma and now (Fig.1).

A snow-wedge model, often analogously used for fold-and-thrust belts, suggests the northern Potwar Plateau was a strongly tapered fold-and-thrust belt prior to 2 Ma., and after this being pushed along the salt décollement without deformation (Jaume, 1988). A shortening of 9-14 mm/yr was estimated using cross-section shortening, amounting to 20-35% of the total convergence rate between the Indian and Eurasian plates (Baker et al., 1988; Pennock et al., 1989). Studies based on seismic reflections estimate a shortening of 7 mm/yr (Pennock et al., 1989) to 18 mm/yr (Jaswal et al., 1997). It has also been suggested that the salt permits the foldbelt to be much wider in map view, with a low-angled (1-3°) cross-sectional taper (Davis and Lillie, 1994). This allows for a low-friction environment for the Salt Range thrust. The deformation across this wide zone can also be correlated to the period of strong sedimentary accumulation between 5 and 1.9 Ma which comprises mostly the Soan formation (Grelaud et al., 2002).

Methodology

In April 2017, a fieldwork was performed aimed at collecting samples from two formations of the Siwaliks, the Soan and the Dhok Pathan. Acquiring the samples in the Soan formation was done with the goal of acquiring a magnetostratigraphic correlation, whereas the samples from the Dhok Pathan formation had the aim to provide vertical-axis rotations of the locations.

Field procedures

All samples were acquired using a gasoline-powered or a battery powered drill, depending on the fragility of the rock. As the formations proved fragile and soft, air was used to cool the drilling bit instead of water. This proved most reliable to prevent the cores from breaking or turning into mud. The orientation of the specimens and the bedding was taken for every site, along with the approximate distance to the previous site, GPS data and lithostratigraphic details. All cores were taken to the Paleomagnetic Lab of Utrecht University. They were cut into standard specimens with a length of 22mm for further analysis.

We collected 122 cores from 28 levels from the Soan formation, in a range of about 3 km, starting South of the village of *Dhari Rai Ditta* towards the village of *Mujahad* in the North of the Potwar Plateau. A minimum of three cylindrical cores (ø = 25mm) were taken from every red-siltish bedding found in succession. The base of the section is just above the unconformity found at the top of the Dhok Pathan formation. The Dhok Pathan was indeed found sharply inclined at about

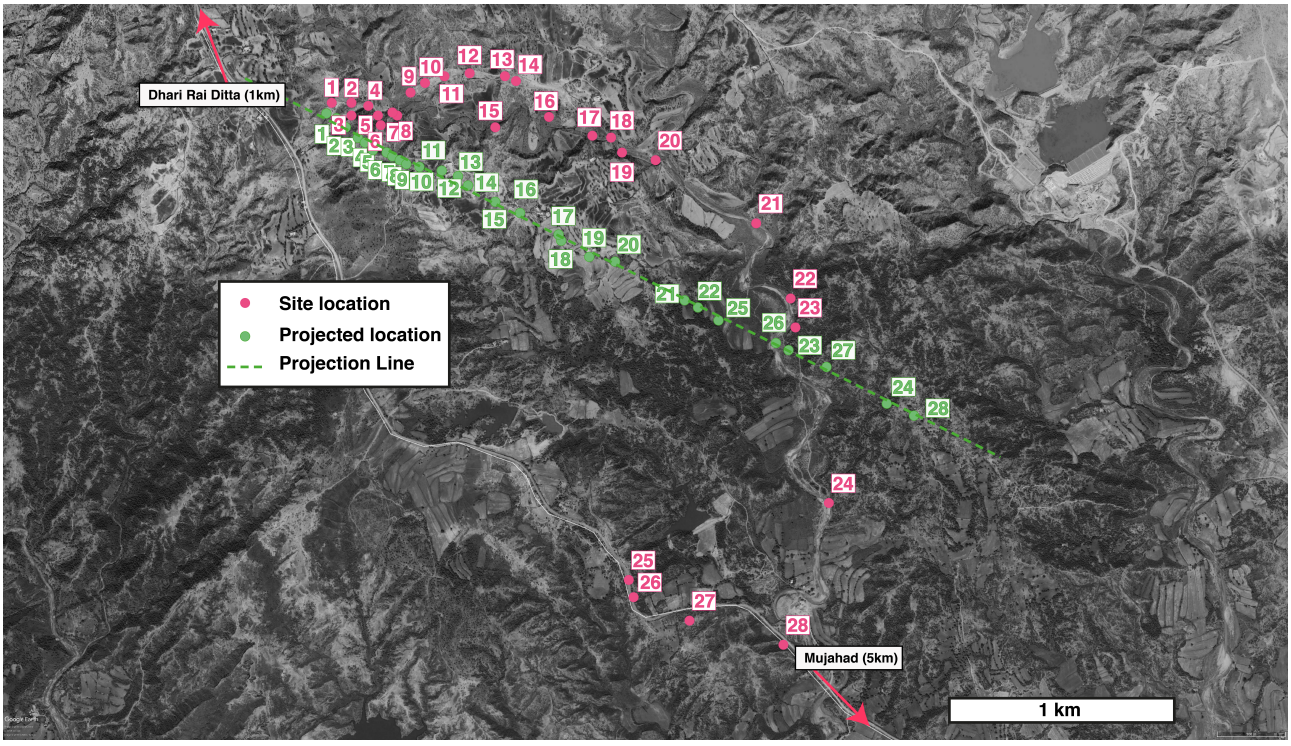

Figure 3 Sites of the Soan formation projected along a best-fitting line using GPS coordinates.

70° with respect to the Soan formation. The section was not continuously exposed and successive sites were sampled roughly perpendicular to the strike of the bedding, later projected along a straight line using the GPS coordinates of each site. Field observations also showed a regular pattern of deposition and no large fluctuations in sedimentations rates are expected.

Using the average bedding plane of the sites, a projection line (Figure 3) was made with a site distance of 30-40m a site, decreasing along the line up to several hundreds of meters between specific sites from 24 to 28. The projection line provides a successive set of sites through time which can be used for magnetostratigraphic dating. The dataset from the Soan formation can also be used to determine vertical-axis rotation, adding a rotational dataset to the Northern Potwar Plateau.

The older Dhok Pathan formation was sampled throughout the Western Potwar Plateau. In total, 301 cores were taken from 24 sites. One of these sites (DP12) turned out to be from the Chinji formation. The formation was often exposed in present river beds which were abundant in the plateau. Creating localities from multiple sites in a specific radius (e.g. <500m) areas proved difficult as the sites can be up to 20 km apart. When possible, at least 12 cores were taken from each site, preferably spread out over several meters. The dataset adds to existing data from literature as it covers the central as well as the western of the Plateau.

Lab procedures

To obtain the ChRM (Characteristic Remanent Magnetisation) of a sample, they were step-wise demagnetised using AF (Alternating Field) and thermal demagnetisation. AF demagnetisation was performed using an in-house developed robotised system (Mullender et al., 2016), using the following demagetisation steps (in mT): 0,5,10,15,20,25,30,35,40,45,50,60,70,80,90,100. Thermal demagnetisation was done in a magnetically shielded oven, using the following steps (in °C): 0, 50, 100, 150, 200, 250, 300, 350, 400, 450, 500, 540, 580, 620, 660. In some cases 50° was skipped as the specimens showed a very strong signal and not all samples were heated up to 660° when they had lost their remanent magnetisation at lower temperatures. For every AF and temperature step, the NRM (Natural Remanence Magnetisation) was measured on a 2G Enterprise horizontal cryogenic magnetometer equipped with three DC squids (noise level 3×10^{-12} A·m^2).

Demagnetisation measurements were analysed plotting the principal components on a Zijderveld diagram (Zijderveld, 1967). Declinations were corrected for the IGRF (International Geomagnetic Reference Field) of -2°. The ChRM plots are analysed with care to disregard secondary signals such as the overprint of the recent GAD (Geocentric Axial Dipole) field and isolate the primary ChRM.

Less straightforward samples, e.g. those wit a large recent overprint, were interpreted using great-circle analysis (McFadden and McElhinny, 1988) to obtain a final paleomagnetic direction (e.g. Figure 4e). In this procedure, the plains through low-coercitivity components and the origin share

the same vector which is a higher-coercivity component. Intersections of planes (visualised by great-circles) can indicate the ChRM of the sample. If possible, a normal or reverse set-point was used which provided great circle solutions using an iterative procedure. ChRM's for each sample are combined into a site-average providing a paleomagnetic direction for further analysis.

Diagram analysis and Fisher statistics are performed using the open-source browser-based portal *paleomagnetism.org* developed by Utrecht University (Koymans et al., 2016). The portal also provides options to analyse magnetostratigraphic sections and orocline formation (Meijers et al., 2017). Literary data was parameterised from available distribution values providing the paleomagnetic directions from the specific study along with the error (Deenen et al., 2011). The coordinate bootstrap reversal test (Tauxe, 2010) was was performed when combining normal and reverse datasets.

A selection of samples from each site was used for AMS (Anistropy of Magnetic Susceptibility) measurements using an AGICO MFK1-FA using Jelinek statistics (Jelínek, 1997). The magnetic susceptibility is semi-automatically measured in 15 directions resulting in a susceptibility tensor where the principle susceptibilities can be correlated to the principal stress axes (Borradaile and Jackson, 2010), providing a tool to isolate a specific tectonic environment within a site or locality.

Results

Soan formation

From the Soan section, 104 specimens from 28 sites were demagnetised where 8 specimens demagnetised with AF and further demagnetised using heating steps. The samples in the Soan formation showed a large variety in terms of quality.

Most of the samples showed a gradual decay up to 70 mT (AF) or 620°C (Thermal), indicating most samples in the Soan formation contained magnetite and likely also maghemite (Figure 4a). Others were not fully demagnetised (>50% left) at 100 mT/660° which is an indication of hematite (Figure 4b,c,d). AF demagnetisation generally provided more stable, but not fully demagnetised results. This is in contrast with thermal demagnetisation, which resulted in a more demagnetised sample, but a more unstable pattern especially visible on low-intensity samples containing hematite. The heating of the samples results in a magnetic component induced in the oven affecting the ChRM of the sample when containing hematite. This was countered by turning the

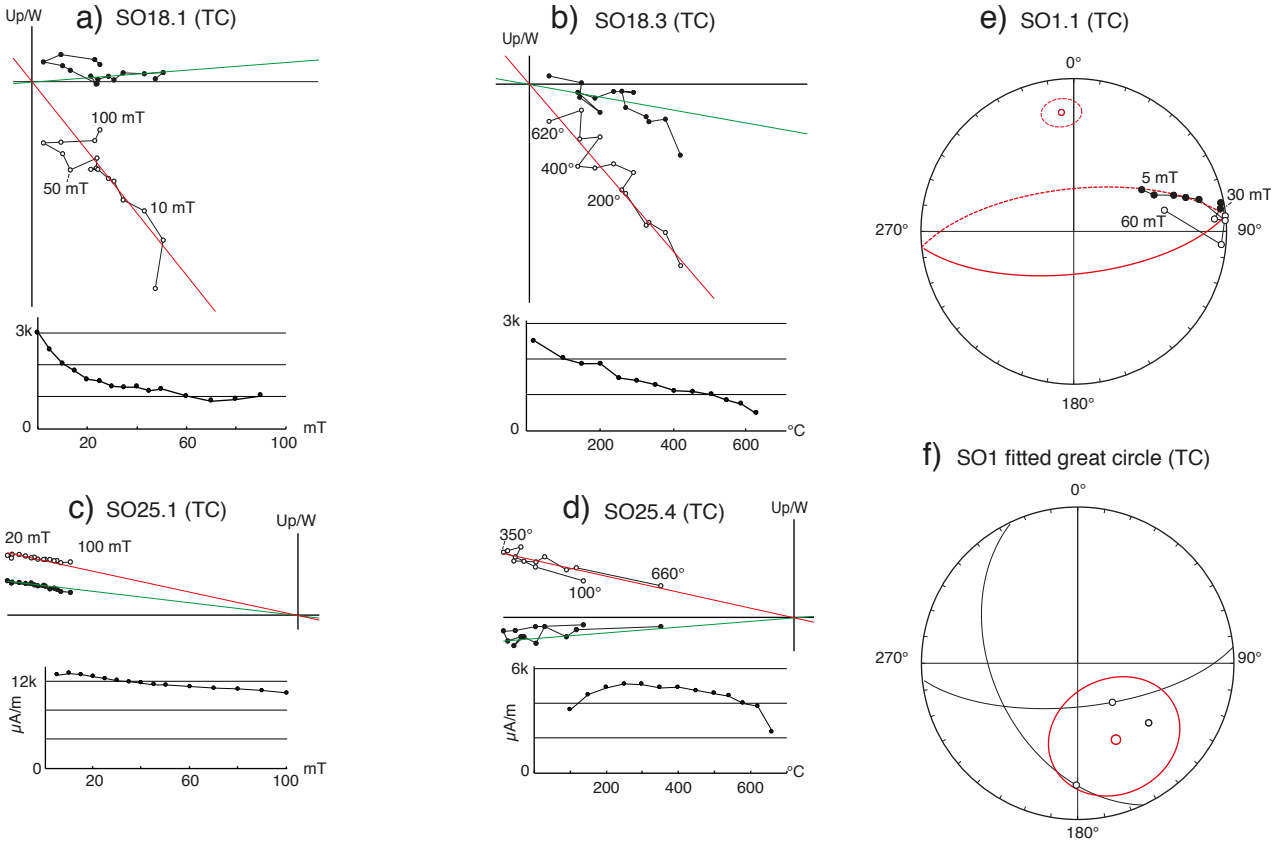

Figure 4 Representative demagnetisation results from the Soan formation. a) Not fully demagnetised sample by AF shows clustering towards the origin at higher coercivitie, b) Similar composition nearly fully demagnetised at 620° but showing alternating pattern from induced field in the magnetically shielded oven, c) Hardly demagnetised hematite during AF demagnetisation, d) Still not fully demagnetised hematite during thermal demagnetisation, however the ChRM is very distinguishable, e) Great-circle analysis on a specific sample, f) Resulting site-average using great-circle analysis providing a clear reversed polarity but no usable declination data.

specimens around 180° every next demagnetisation step, resulting in the alternating pattern (Figure 4b).

Magnetostratigraphy

A positive inclination can be considered a normal magnetic field whereas as a negative inclination indicates a reversed magnetic field. The samples were mainly interpreted to assess which polarity

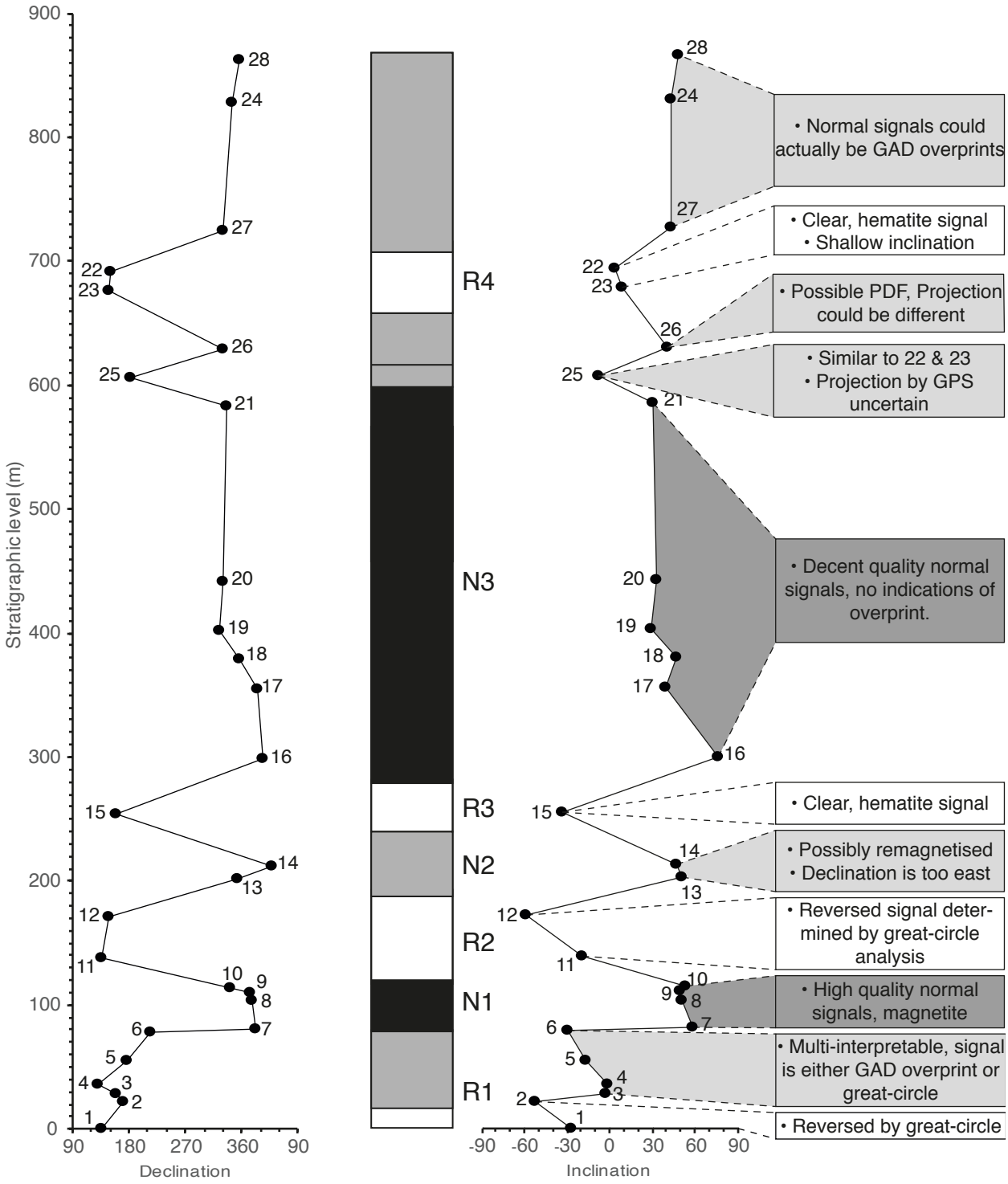

Figure 5: Preliminary magnetostratigraphic column for the Soan formation showing the declination and inclination of each specific site along the stratigraphic level.

the ChRM showed, and a subset which showed reliable declination values was used for vertical-axis rotation analysis.

Due to the small rotation in the area a present-day GAD field overprint is not always distinguishable from a true normal component. A ChRM around 0° declination, 51° inclination can indicate a GAD overprint, a true normal polarity, or if the distribution is on a specific plane, it can be used to infer a reverse polarity. This is the case in e.g. site 2 (Figure 5) where polarity is uncertain.

The inclination known for the latitude, ± 51°, can not always be observed due to non-primary signals still affecting the component, or although unlikely, a transitional state of the field. The average declination and inclination of each site are plotted along the stratigraphic level in Figure 5, showing their respective normal, reverse or uncertain polarities.

The magnetostratigraphic column shows 4 definite reversals defining 2 normal and 3 reversal zones, with the possibility of 4 more reversals in the full section. The samples density is highest at the base of the section, where a clear reversed zone is seen. Approximately 80m higher in the section there is a clear normal zone (80-120m). Lower site density follows, but a clear alternating sequence of declination (from ~150° to 30°) and inclination changes (from -60° to +60°) show a clear reversal sequence. This is followed by a very long (300-600m) period of normal polarity. The top 300m of the column has a lower site density and the sites are projected along a larger distance which increases the likelihood of misplacement on the projection line. They show a normal polarity but these could be misplaced within the column. Site 25 shows a very convincing reversed polarity but its stratigraphic level is debatable.

No positive reversal test (Tauxe, 2010) (N_1 = 48, N_2 = 36, Angle between directions: 153.09) was found as most reversed samples tended to have a more shallow inclination.

Dhok Pathan formation

The specimens from the 23 sites of the Dhok Pathan formation and 1 site from the Chinji formation (site 12) provided 301 measurements from which 204 ChRM's were obtained after selection (Table 1). All Dhok Pathan samples were heated up to 150° prior to AF demagnetisation to eliminate the maghemite shell sometimes present on magnetite grains (van Velzen and Zijderveld, 1995), which provided more stable results. Some samples show a randomly magnetised component while subjected to the AF above 45 mT, known as a gyro-remanent magnetisation (GRM) (Dankers and Zijderveld, 1981). It renders higher coercivities unusable and low coercivities up to 40 mT often indicate the GAD overprint. Similar to the Soan formation, the directions found in the Dhok Pathan samples were often indistinguishable from the present-day GAD field, All samples combined indicate a combined declination mean of 357.8° ± 3.5° which is in the same range as the GAD field in Pakistan (Table 1).

Most of the samples showed a combination of magnetite and hematite as carriers of the primary signal. Mineralogy also appeared to be similar to the Soan formation, where magnetite and

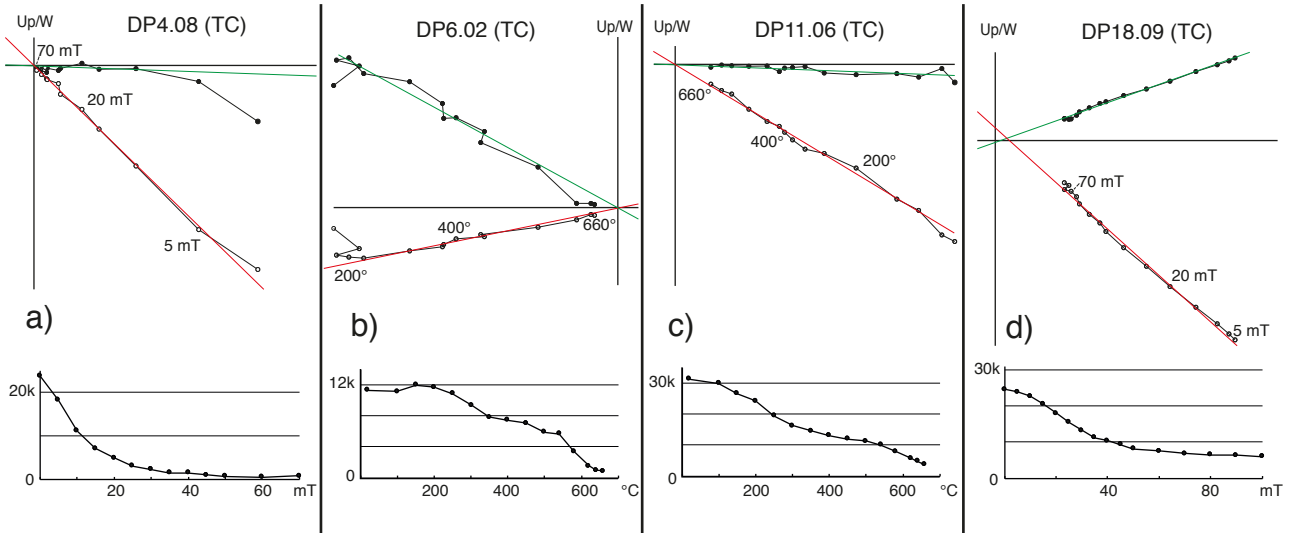

Figure 6: Representative demagnetisation results from the Dhok Pathan formation. a) Fully demagnetised magnetite by AF showing a clear ChRM, b) Demagnetisation of magnetite showing a significant drop at 580°, c) Demagnetisation of magnetite with remaining hematite signal. The magnetic direction of both minerals is not distinguishable, d) AF demagnetisation not further demagnetising after 50 mT, a clear indication of hematite.
Figure 7: Vertical-axis rotations of localities and remaining sites after bedding correction.

Table 1 Paleomagnetic results of the Dhok Pathan formation after bedding correction and IGRF correction. Not bold = rejected data, bold = used for further analysis.

	N	N_{45}	D	I	ΔD_x	ΔI_x	k	α_{95}	K	A_{95}	Bedding
DP01	10	10	142,1	-55,4	19,3	15,3	12,1	14,5	10,6	15,5	*N/A*
DP02		***No usable data***									
DP03	6	6	359	-45,7	9,0	9,8	86,3	7,3	71,2	8,0	056/05
DP04	9	9	358,2	48,2	6,3	6,5	102,6	5,1	80,0	5,8	276/03
DP05	5	5	357,4	-61,9	10,3	6,2	207,4	5,3	105,3	7,5	*N/A*
DP06	11	11	349,5	-43,5	6,0	7,6	64,1	5,7	63,0	5,8	204/07
DP07	11	11	341,9	62,0	11,5	6,9	59,3	6,0	31,7	8,2	140/05
DP08	11	11	358,1	39,0	8,4	10,9	37,5	7,6	35,5	7,8	*N/A*
DP09		***No usable data***									
DP10	8	8	3,4	-12,3	10,4	18,3	21,6	12,2	30,7	10,2	245/10
DP11	12	12	7,5	43,6	6,7	7,8	67,3	5,3	52,0	6,1	*N/A*
DP12	5	5	5,6	-38,4	4,8	6,4	195,8	5,5	234,0	5,0	265/07
DP13	12	12	7,5	50,3	9,3	8,9	41,9	6,8	30,5	8,0	*N/A*
DP14	13	13	332,6	49,4	7,9	7,7	59,4	5,4	38,1	6,8	*N/A*
DP15	12	12	17,3	39,1	6,5	8,5	53,2	6,0	52,7	6,0	*N/A*
DP16	12	12	23,5	4,2	3,2	6,4	142,1	3,8	184,5	3,2	307/03
DP17	6	6	308,1	-49,7	14,1	13,6	44,3	10,2	31,7	12,1	*N/A*
DP18	13	13	345,9	52,3	5,2	4,7	114,5	3,9	89,7	4,4	*N/A*
DP20	16	16	347,5	41.0	3.9	4.9	109.8	3.5	104.8	3.6	277/14
DP21	11	11	359,7	24.0	5.4	9.3	41.8	7.1	75.4	5.3	265/09
DP22	4	4	1,0	27.6	5.0	8.1	350.8	4.9	363.6	4.8	276/18
DP23	5	5	6,8	55.9	17.2	13.4	38.5	12.5	31.9	13.8	*N/A*
DP24		***No usable data***									
DP25	12	12	349,4	39.2	4.2	5.5	70.1	5.2	125.2	3.9	301/05

Table 2 Rotational Localities after bedding correction

	N	N_{45}	D	I	ΔD_x	ΔI_x	k	α_{95}	Source
Chhab	20	20	357,3	52,2	5,1	4,5	74,2	3,8	**This paper**
Danda Shah	32	32	3,8	38,7	5,7	7,4	16,7	6,4	
Talagang	35	35	347,7	51,4	5,6	5,2	31,6	4,4	
Soan	42	40	340,4	37,6	6,9	9,2	10,3	7,4	
Pabbi Hills	89	86	354,5	41,5	3,0	3,7	24,3	3,2	**Keller et al., 1977**
Dhok Pathan	127	127	354,2	49,8	5,1	5,0	10,3	4,1	**Barndt et al., 1978**
Rohtas	42	38	349,7	35,1	6,8	9,6	12,4	6,9	**Opdyke et al., 1979**
Mangla Samwal	52	46	357.6	39.5	5.1	6.6	19.8	4.9	
Chambal Ridge	49	49	355.5	28.9	4.6	7.3	20.4	4.6	
Kotal Kund	66	66	322,6	34,7	4,1	5,8	19,8	4,0	**Opdyke et al., 1982**
Dhala Nala	37	37	322,2	32,6	6,2	9,2	15,4	6,2	
Tatrot	45	45	331,6	33,4	4,3	6,4	25,4	4,3	
Chakwal Baun	25	25	332,3	34,0	7,6	11,0	15,8	7,5	
Nagri	26	25	355,4	36,7	7,2	9,8	17,5	7,1	
Dhaud Kel	4	4	348,2	39,7	9,6	12,3	108,4	8,9	
Kaulial Kas	45	45	349,3	39,9	5,9	7,5	17,1	5,3	**Tauxe & Opdyke, 1982**
Malawalla Kas	35	31	352,1	24,9	7,0	11,8	10,4	8,4	
Bora Kas	49	48	349,3	39,9	6,0	8,7	17,1	5,3	
Rhata Kas	39	36	330,6	36,8	7,7	10,5	11,8	7,3	

hematite or a combination thereof make up nearly all primary ChRM's.

Samples which have a ChRM purely in hematite provide a very reliable direction (e.g. DP12,16,18), whereas samples containing a drop in intensity common for magnetite sometimes contained a less reliable signal. Thermal alteration in the oven also affected the stability of the readings. This resulted in a larger uncertainty (e.g. site DP7) or a near-random distribution (DP2,9,24), in which case the results were unusable.

Vertical-axis rotation

Site averages for the Dhok Pathan formation are provided in Table 1. The sites show a contrasting pattern throughout the plateau with rotations ranging from 28° CCW (DP14) up to 23° CW (DP16). The Dhok Pathan formation was usually found at a near-horizontal bedding, therefore it is assumed all rotations are rotations along a vertical axis.

Sites within a radius of ~10 km were combined into localities (Table 2). DP3, 4 and 5 have been combined into the *Chhab* locality, DP10, 11 and 13 make up the *Danda Shah* locality. DP7 and 8

were combined into the *Talagang* locality. Previously acquired data used in this research are also included in Table 2.

The *Chhab* and *Danda Shah* localities show no rotation for the west of the plateau (Figure 7), in contrast with the Dhaud Kel locality from published data (Fig. 1, 11), which shows a 12° CCW rotation at the Kalabagh fault in the far west (Opdyke et al., 1982). DP12 (Chinji Formation) also shows an absence of rotation. The Central Potwar plateau has on average a CCW rotation, but shows to large inconsistencies. Several locations did not contain any usable demagnetisation data (DP2, 9,17) and were rejected for further analysis. Two pairs (DP14-15 and DP16-17) show very different results despite being extremely close. DP 14 and 15 combined show a strongly elongated distribution which is not possible to represent secular variation. This can be the result of remagnetisation of one or both of the sites or errors made in the field. These sites are omitted from

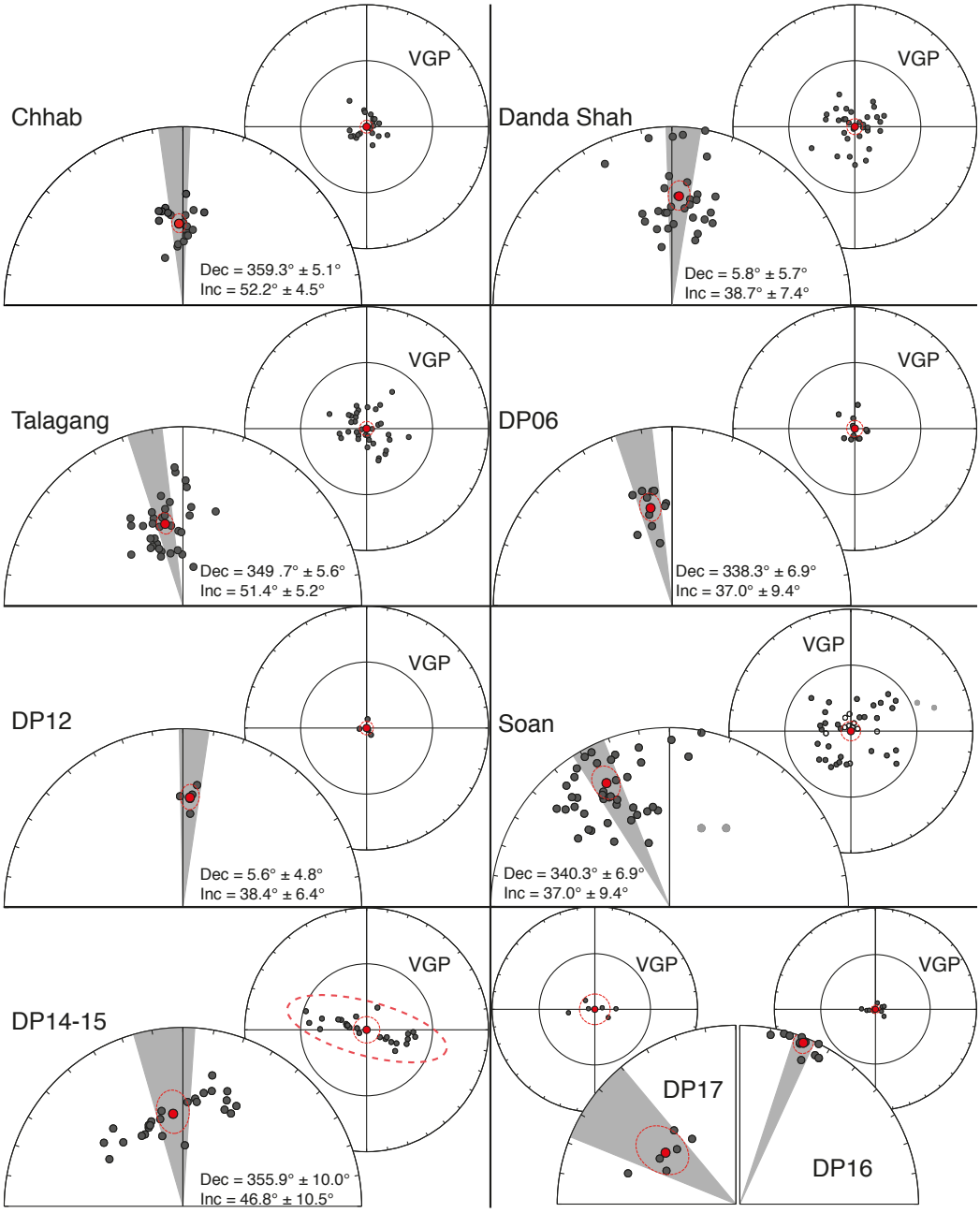

Figure 7 Vertical-axis rotations of localities and remaining sites after bedding correction.

further analysis. DP16 and 17 show extremely different rotations deemed impossible at this scale. The remaining sites show that the Dhok Pathan formation has an approximate 10° CCW tectonic rotation in the Central Potwar plateau based on DP6, 20 and the Talagang locality, in good agreement with literature data from the near-region.

The ChRM's of the Soan section can also be combined into a single rotation locality (Figure 7). Although the normal and reverse distribution showed no positive coordinate bootstrap reversal test, combining them could average out the shallow inclination in the reversed section and provide a better indication of the declination. The mean direction of the primary signal has been measured at 353.3° ± 6.1° (k = 9.7 α_{95} = 5.4).The final shallow inclination (45.0° ± 7.8°) can be attributed to the shallow reversed data points (37.2 ± 21.2) found in the section. These can be affected by a non-primary signal, mainly the current-field overprint in reversed signals, resulting in shallower inclinations. The vertical-axis rotation of 19.5° CCW is consistent with literature data in the Northern Potwar Plateau (Tauxe & Opdyke, 1982).

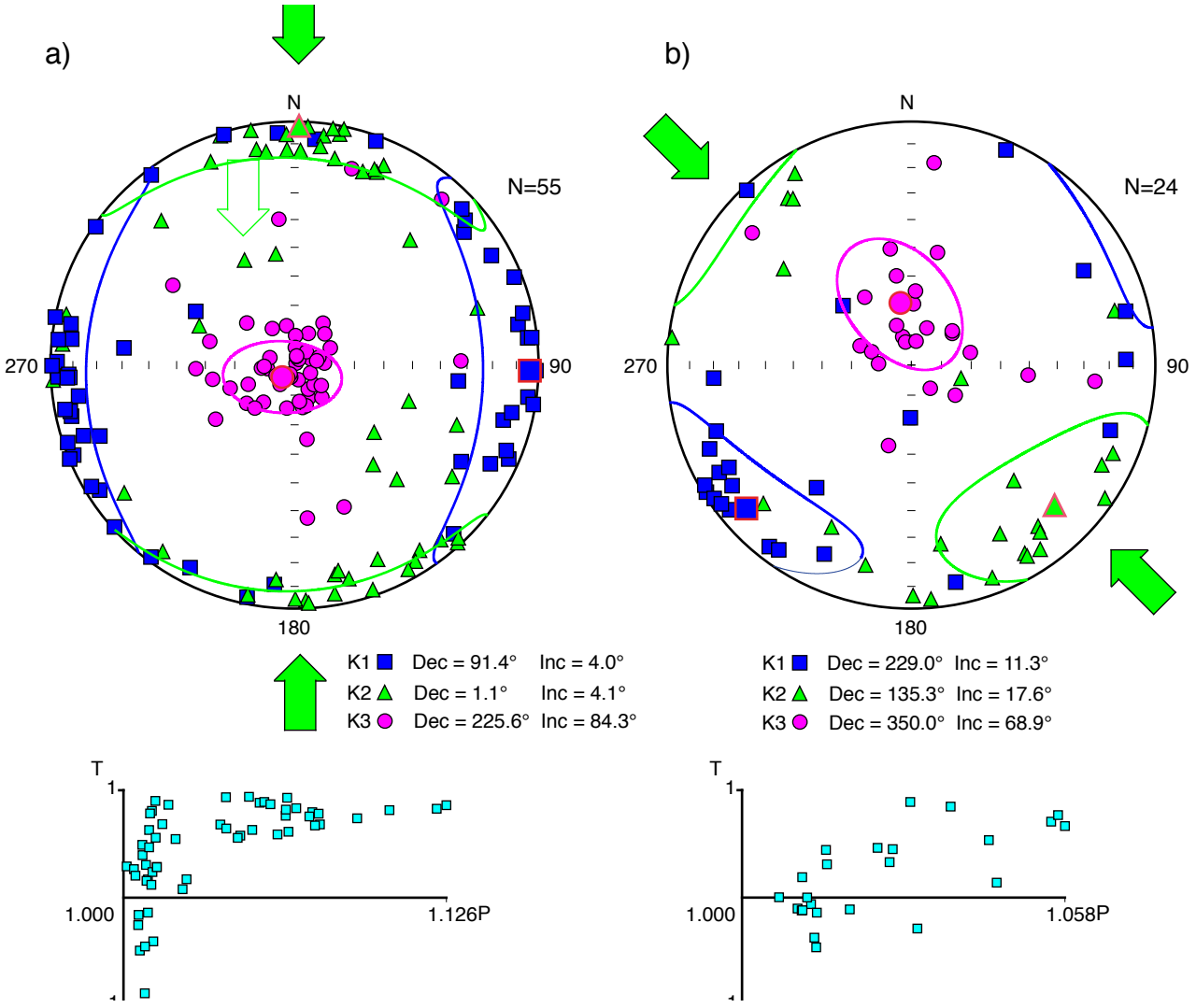

Figure 8 Anisotropy of the magnetic susceptibility after tectonic correction found in the a) the Dhok Pathan formation shows a N-S compressional axis and b) the Soan formation shows a NW-SE compressional axis.

Anisotropy of magnetic susceptibility (AMS)

The primary axes of the magnetic susceptibility show κ_1 and κ_2 to be horizontal after tectonic correction and by default perpendicular to each other, with κ_3 perpendicular to the bedding and vertical within error (Figure 8). The maximum principal axis of the susceptibility relates to the minimum principal axis of the stress tensor, and vice versa. The maximum principal axis of the susceptibility axis κ_1 therefore indicates a stress state of extension. Both κ_2 and κ_3 therefore indicate compression, where κ_3 is the effect of compaction of the sediment after deposition. Axis κ_2 can be related to a horizontal compression if the inclination is very low, which is the case as observed in Figure 8. The error ellipses are large but do not overlap, indicating a sufficient anisotropy in the magnetic susceptibility. This therefore indicates a North-South (001°/181°) compressional axis, in agreement to the stress environment of the Himalayas in this region.

The Soan formation however, shows a 135°/3315° compressional axis and 49°/229° extension. The ellipsoids are relatively small and the axis κ_3 is perpendicular within error. There is also a slightly higher inclination (11.3°-17.6°). Along with a bedding dip of ~18° SE the area and the average strike of the Soan formation (26°) and the local orientations and large faults (e.g. the axis of the Soan syncline at 30°) matches these orientations approximately.

Discussion

Age the Soan formation

From Figure 5 clear reversed intervals can be observed at the bottom of the section, at sites 1 (R1), 12 and 13 (R2) and 15 (R3), a normal interval at sites 7-10 (N1), and an ambiguous normal interval at sites 13-14 (N2). A clear normal field (N3) is observed in sites 16 to 21, albeit there is a large gap of ~100m from 20 to 21. The top (R4) has a clear reversed section at site 22 and 23, but arguable intervals in the rest.

The problems with the results are the following. 1) The large gap between 20 and 21 could still contain a reversal, 2) R4 has a strong reversed ChRM section but the normal fields are possibly overprints of the GAD field, 3) N2 could actually be an overprint of the GAD and 4) site 2-6 could both be a normal and reverse polarity (Figure 5).

The generally assumed interval of Upper Pliocene - Lower Pleistocene taken provides a range of 1 to 2.5 myrs for the total timespan of the section, indicating a sedimentation rate of 29 to 86 cm/kyr for the 862m long section. This agrees with the highest sedimentation rate of the Dhok Pathan formation observed at 79 cm/kyr (Johnson et al., 1985). The large normal interval N3 is estimated

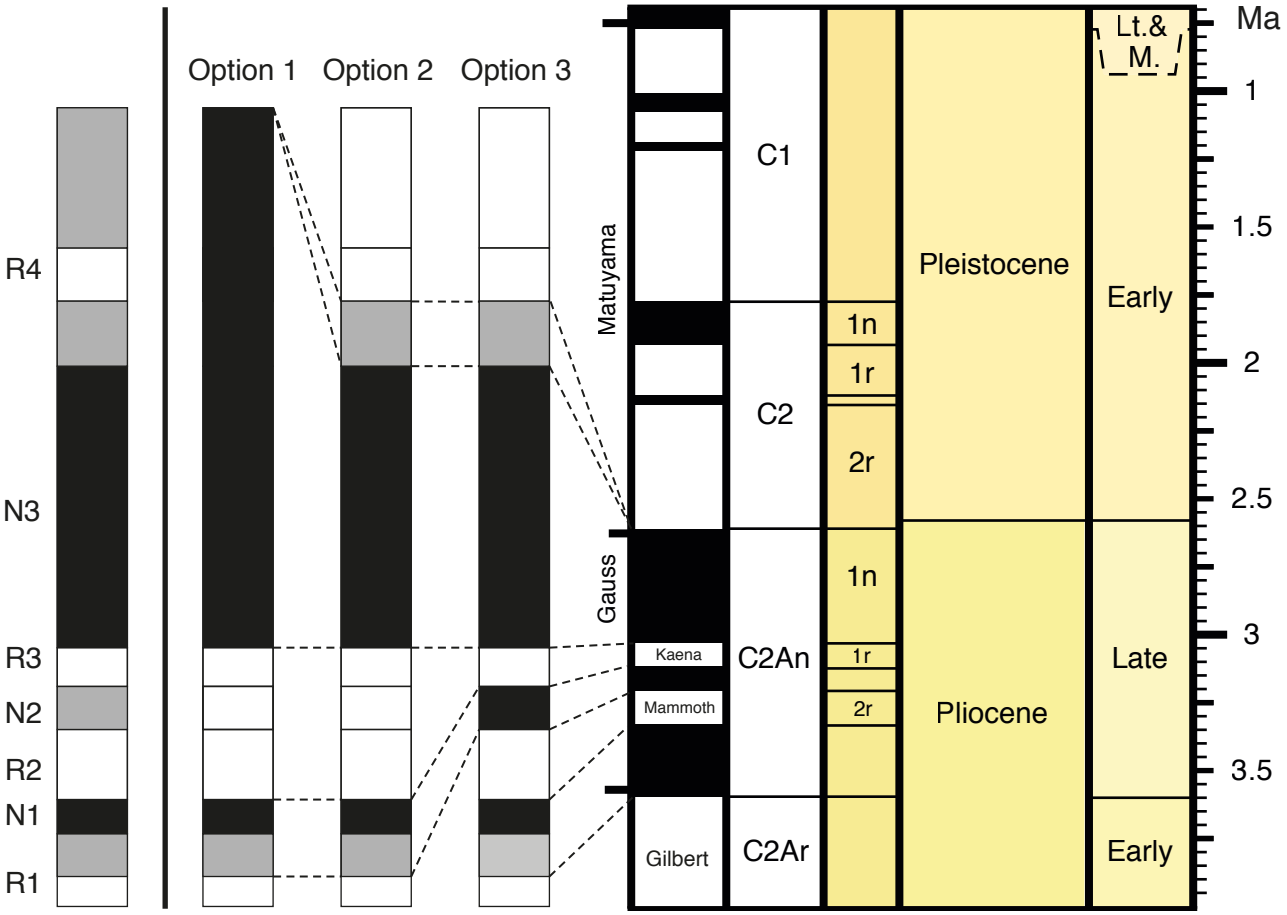

Figure 9 Options of the magnetostratigraphic column of the Soan Formation fitting the GTS (Geomagnetic Time Scale). N3 is always correlated to the Gauss chron, providing a baseline.

at approximately 276m, therefore the interval would have a time-span between 320 and 951 kyrs. The only normal chron known of that length at the time is in the top of the Gauss normal interval (C2An.1n) at 451 kyrs, also indicating the boundary between Pliocene and Pleistocene. Hypothesising the large gap in the sampling contains a reversed field would make the normal chron approximately 150m (Figure 9), therefore 160 to 476 kyrs in terms of time. This can still indicate the Gauss chron, but leaving no match for the Matuyama (C2r.2r) in this section. If it is C2An.3n, there is no reversed interval matching C2Ar at the bottom of the section. It can therefore be concluded that as a baseline, N3 can be correlated to the Gauss Chron with the Kaena (C2An. 1r) below.

This leaves the top of the section with three possibilities. A much longer Gauss chron (Option 1), would require a significant increase in sedimentation rates (Figure 10) up to 190 cm/kyr, which is highly unlikely considering the upper boundary of 86 cm/kyr. A slightly longer Gauss chron with a short R4 can not be matched to the GTS. A larger R4 as depicted in Option 2 and 3, can easily be matched to C2r.2r.

The bottom section has several possibilities. An extra normal interval N2 between R2 and R3 and a longer N1 (Option 3) would correlate N1 to C2An.3n. An obscured reversed state in-between R2 and R3 would correlate N1 to C2An.3n. The length of R1/N1 can be either, but has no implications for the magnetostratigraphic correlation.

Sedimentation rates agree most with a longer N1 in combination with a normal interval N2 between R2 and R3. Option 3 shows the most consistent rates where the first two scenarios show a very high sedimentation rate at the Plio-Pleistocene boundary of approximately 190 cm/kyr. Option 1 furthermore shows a highly fluctuating sedimentation rate. Option 1 and 2 would place the base of the Soan formation at approximately 3.2-3.3 Ma, but is deemed more unlikely as field observations

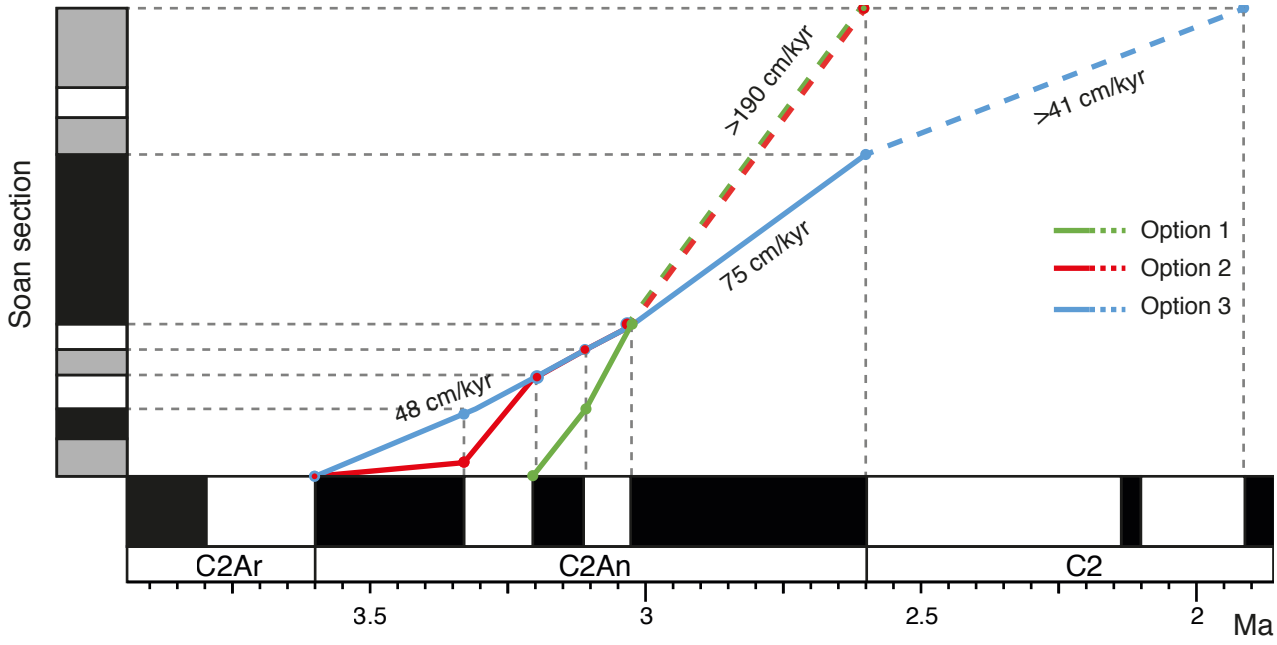

Figure 10 Sedimentation rates of the three options for the magnetostratigraphic correlation. Dotted lines are projected according to the thickness of the top interval of the measured section. Real sedimentation rates can be higher, not lower.

and literature do not support these scenarios. The base of the Soan formation is therefore placed in the C2Ar (Gilbert) chron at around 3.7 Ma as extrapolated from this section.

This shows sedimentation rates have also increased from the Pliocene (Figure 10). Sedimentation rates up to 30 cm/kyr have been observed in the Nagri formation where an increase in tectonic activity was also observed (Johnson et al., 1985). It is not a surprise that the displacement of the evaporites has also led to higher sedimentation rates. The magnetostratigraphic results suggest a sedimentation rate of ~ 40 cm/kyr at 3.5 Ma up to 75 cm/kyr in the Late Pliocene.

Vertical-axis rotation of the Potwar Plateau

There is however a rather coherent rotational pattern throughout the Potwar Plateau. The CCW vertical-axis rotation of approximately 20° in the North observed in the Dhok Pathan formation matches the rotation of the Soan formation as well as site DP23, although the dip of the Dhok Pathan formation is up to 80° inclined with respect of the Soan formation. This suggests a tectonic age younger than 3.7 Ma for the rotation of the Soan formation observed in the North of the Plateau. This is in contrast with the Western Plateau which shows no rotation since Upper Miocene, based on DP21,22,25 and the Chhab and Danda Shah localities (Figure 11). The central plateau shows a slight CCW rotation of approximately 10° based on the Talagang locality and single sites DP6, 12 and 20. This corresponds with a larger rotation (up to 30°) from (Tauxe and Opdyke, 1982) a little more the East. Rotation along the Eastern Salt Range is more significant —

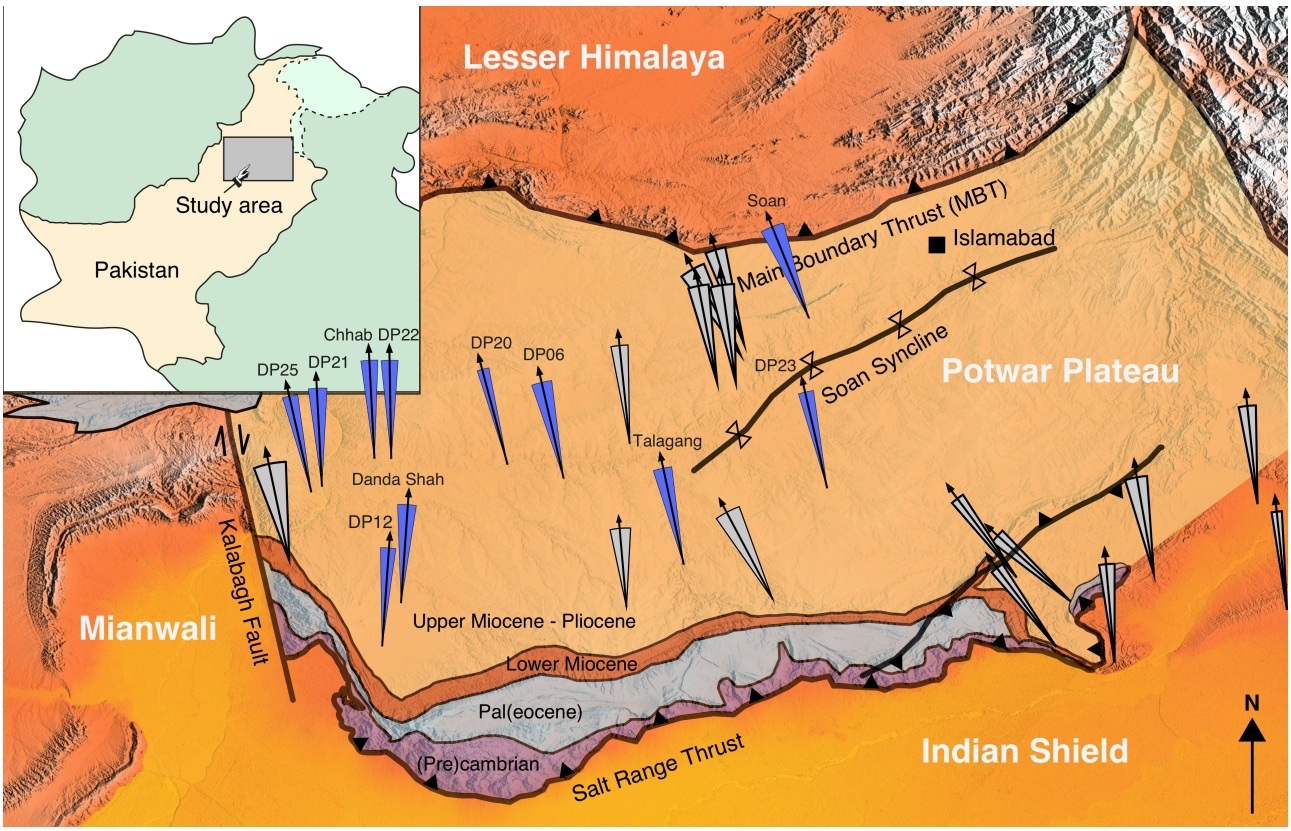

Figure 11 Newly added localities and sites (dark blue) providing vertical-axis rotations of the interior of the Potwar Plateau along with previously presented literary data (grey, see Figure 1).

always CCW up to 35° but shows no correlation with the interior. The general trends suggest a differential vertical-axis rotation within the plateau where the Western Plateau has no rotation and the Central Plateau has a CCW rotation.

This is supported by the Talagang locality and sites from Tauxe and Opdyke (1982) Local geological features are also more prevalent in the East and the Northern plateau than in the West, e.g. the orientation of the Soan syncline of about 30°. The 135°/315° compressional regime can be interpreted as a rotation of 30° from the expected N-S compressional regime of the India-Eurasia collision. This is assuming the anisotropy in the magnetic susceptibility formed due to the strongest stress-regime present, the India-Eurasia collision. If the anisotropy formed due to a more recent stress-field, a current 330°/150° could be suggested for the compressional direction fo the Eastern Potwar Plateau. In both cases, the average of the Dhok Pathan formation, mostly sampled in the Western and the Central plateau showed a contrasting near-perfect North-South (1°/181°) compressional regime, supporting either differential rotation in the area or a differential stress regime.

Geological Implications

The rotations of the Potwar Plateau show a positive regression analysis with respect to the surrounding structures (Figure 12). This would suggest an orocline within the Potwar plateau. This structure was formed within the last 2.1 Myr as it includes the Soan syncline where its base was dated at 3.7 Ma and the structure itself was estimated to have formed 2.1 Myr ago (Johnson et al.,

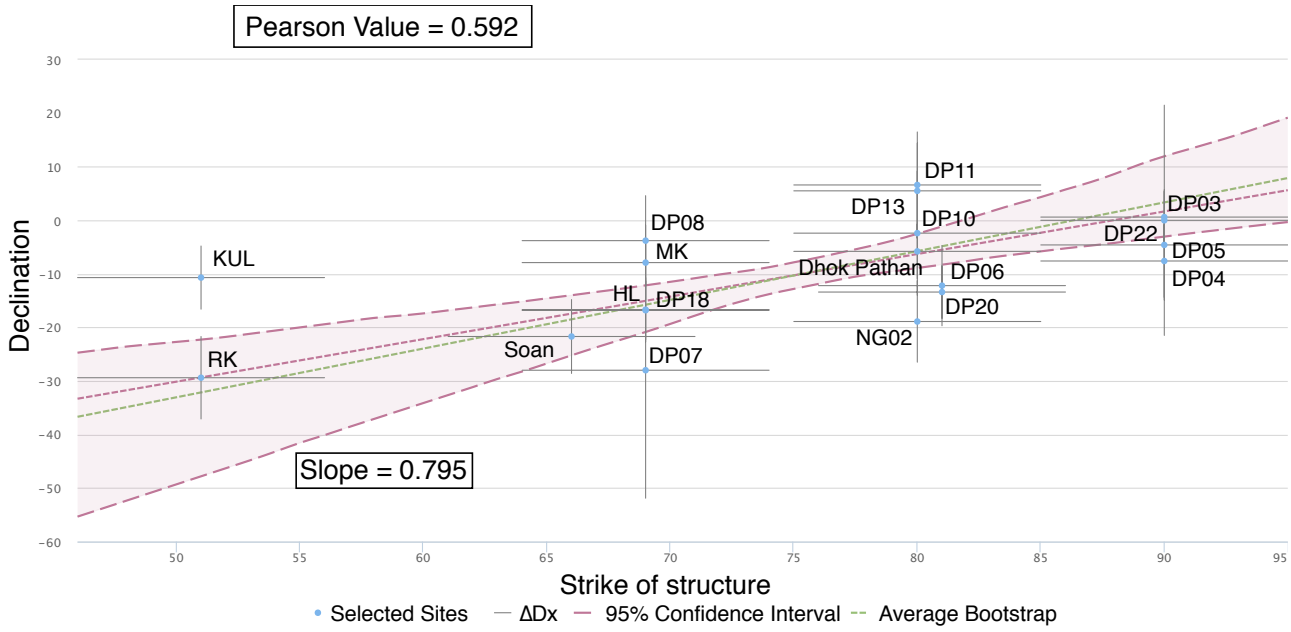

Figure 12 Regression analysis of the orientation of the structure and the observed rotations in the Potwar Plateau, also known as the Orocline Test. Pearson value of 0.592 is significantly higher than the 99% confidence value for N = 19 (0.528) (Pastor-Galán, 2017).

1986). This correlates to the approximate age of the Salt Range ramping event at 2.2 Ma, suggesting a single deformation phase for the Soan Syncline and the orocline. The absence of

rotation in the Western Plateau, suggests the Mianwali re-entrant is no orocline on its Eastern side and the Kalabagh Fault shows a near-perfect dextral strike-slip motion and accommodates a large amount of displacement (80 km), in contrast with CW rotations observed in (Opdyke et al., 1982), which are likely affected by the proximity to the fault itself. This enabled the Western Plateau to move in a southward motion along the Kalabagh Fault into the Salt Range Thrust. The Kalabagh Fault is most likely an accommodation feature caused by less subsurface salt, resulting in significantly more basal friction and restricting southward movement of the front. The Salt Range Thrust begins at the Southern end of the Kalabagh Fault, suggesting an age between 10 and 2.2 Ma. This is in agreement with the estimated shortening between 700 and 1400 cm/kyr in the Potwar Plateau, which suggests an existence of about 9 Myrsfor the 80km long fault. As the Western Salt Range also exposes the larger part of the evaporite substrate, a prevalence of the evaporites in the subsurface mostly in the Western part of the plateau would enable a low-friction environment to enable this amount of displacement.

Less significant thrusting is observed towards the east of the Salt Range Thrust, which would suggest a higher-friction environment and therefore less significant or depleted evaporite décollement. This can be confirmed by the presence of rotation in the Eastern Plateau, in contrast with the Western part. The significant friction in the East prevent the southward-slip of the Plateau and, anchored to the Western Plateau, slightly rotated CCW by 20-30°.

Conclusion

New and existing paleomagnetic data shows a coherent rotational pattern throughout the Potwar Plateau in contrast with the 0-2° CW rotation of the Indian Plate. This is explained by the evaporite décollement, being present in the Western plateau resulting in a low-friction environment, forming the *Kalabagh Fault*, a dextral fault on the Western margin of the Potwar plateau and showing no significant rotation. A contrasting rotation up to 30° CCW was observed in the Eastern plateau near the Soan Syncline. The rotational difference together with the local structures are part of an orocline within the plateau, indicating a deformation phase dated younger than 2.1 Ma, assumed to be in the same timeframe as the onset of ramping of the Salt Range Thrust. Due to the influence of the evaporite décollement on the Western part of the area, it is suggested that the Potwar Plateau and the Salt Range are a local expression of the India-Eurasia convergence heavily influenced by salt tectonics.

Bibliography

Baker, D.M., Lillie, R.J., Yeats, R.S., Johnson, G.D., Yousuf, M. and Zamin, A.S.H., 1988. Development of the Himalayan frontal thrust zone: Salt Range, Pakistan. Geology, 16(1): 3-7.

Barndt, J., Johnson, N.M., Johnson, G.D., Opdyke, N.D., Lindsay, E.H., Pilbeam, D. and Tahirkheli, R.A.H., 1978. The magnetic polarity stratigraphy and age of the Siwalik group near Dhok Pathan village, Potwar Plateau, Pakistan. Earth and Planetary Science Letters, 41(3): 355-364.

Barry, J.C., Lindsay, E.H. and Jacobs, L.L., 1982. A biostratigraphic zonation of the middle and upper siwaliks of the potwar plateau of Northern Pakistan. Palaeogeography, Palaeoclimatology, Palaeoecology, 37(1): 95-130.

Borradaile, G.J. and Jackson, M., 2010. Structural geology, petrofabrics and magnetic fabrics (AMS, AARM, AIRM). Journal of Structural Geology, 32(10): 1519-1551.

Cotton, J.T. and Koyi, H.A., 2000. Modeling of thrust fronts above ductile and frictional detachments: Application to structures in the Salt Range and Potwar Plateau, Pakistan. Bulletin of the Geological Society of America, 112(3): 351-363.

Dankers, P.H.M. and Zijderveld, J.D.A., 1981. Alternating field demagnetization of rocks, and the problem of gyromagnetic remanence. Earth and Planetary Science Letters, 53(1): 89-92.

Davis, D.M. and Lillie, R.J., 1994. Changing mechanical response during continental collision: Active examples from the foreland thrust belts of Pakistan. Journal of Structural Geology, 16(1): 21-34.

Deenen, M.H.L., Langereis, C.G., van Hinsbergen, D.J.J. and Biggin, A.J., 2011. Geomagnetic secular variation and the statistics of palaeomagnetic directions. Geophysical Journal International, 186(2): 509-520.

Gansser, A., 1981. The geodynamic history of the Himalaya. Zagros Hindu Kush Himalaya Geodynamic Evolution: 111-121.

Gee, E.R. and Gee, D.G., 1989. Overview of the geology and structure of the Salt Range, with observations on related areas of northern Pakistan. Geological Society of America Special Paper, 232: 95-112.

Grelaud, S., Sassi, W., de Lamotte, D.F., Jaswal, T. and Roure, F.o., 2002. Kinematics of eastern Salt Range and South Potwar Basin (Pakistan): A new scenario. Marine and Petroleum Geology, 19(9): 1127-1139.

Jaswal, T.M., Lillie, R.J. and Lawrence, R.D., 1997. Structure and evolution of the northern Potwar deformed zone, Pakistan. AAPG bulletin, 81(2): 308-328.

Jaume, S.C., 1988. Mechanics Of The Salt Range-Potwar Plateau, Pakistan: A Fold-And-Thrust Belt Underlain By Evaporites. Tectonics, 7(1): 57-71.

Jelínek, V., 1997. Measuring anisotropy of magnetic susceptibility on a slowly spinning specimen—basic theory. AGICO print(10): 27.

Johnson, G.D., Raynolds, R.G.H. and Burbank, D.W., 1986. Late Cenozoic tectonics and sedimentation in the north-western Himalayan foredeep: I. Thrust ramping and associated deformation in the Potwar region. Foreland basins, 8: 273-291.

Johnson, N.M., Opdyke, N.D., Johnson, G.D., Everett, H. and Tahirkhelp, R.A.K., 1982. Magnetic Polarity Stratigraphy And Ages Of Siwalik Group Rocks Of The Potwar Plateau, Pakistan. Palaeogeography, Palaeoclimatology, Palaeoecology, 37: 17-42.

Johnson, N.M., Stix, J., Tauxe, L., Cerveny, P.F. and Tahirkheli, R.A.K., 1985. Paleomagnetic chronology, fluvial processes, and tectonic implications of the Siwalik deposits near Chinji Village, Pakistan. The Journal of Geology, 93(1): 27-40.

Keller, H.M., Tahirkheli, R.A.K., Mirza, M.A., Johnson, G.D., Johnson, N.M. and Opdyke, N.D., 1977. Magnetic polarity stratigraphy of the Upper Siwalik deposits, Pabbi Hills, Pakistan. Earth and Planetary Science Letters, 36(1): 187-201.

Khan, M.A., Ahmed, R., HILAL, A.R. and KEMAL, A., 1986. Geology of Petroleum in Kohat-Potwar Depression, Pakistan. The American Association of Petroleum Geologists Biillelin, 70(4): 19.

Klootwijk, C.T., Nazirullah, R. and de Jong, K.A., 1986. Palaeomagnetic constraints on formation of the Mianwali reentrant, Trans-Indus and western Salt Range, Pakistan. Earth and Planetary Science Letters, 80(3-4): 394-414.

Koymans, M.R., Langereis, C.G., Pastor-Galán, D. and van Hinsbergen, D.J.J., 2016. Paleomagnetism. org: An online multi-platform open source environment for paleomagnetic data analysis. Elsevier.

Lillie, R.J., Yeats, R.S., Leathers, M., Baker, D.M., Yousuf, M. and Jaume, S.C., 1985. Interpretation of seismic reflection data across the Himalayan foreland thrust belt in Pakistan. Geol. Soc. Am., Abstr. Programs;(United States), 17(CONF-8510489-).

McElhinny, M.W. and McFadden, P.L., 1998. The magnetic field of the earth: paleomagnetism, the core, and the deep mantle, 63. Academic Press.

McFadden, P.L. and McElhinny, M.W., 1988. The combined analysis of remagnetization circles and direct observations in palaeomagnetism. Earth and Planetary Science Letters, 87(1-2): 161-172.

Meijers, M.J.M., Smith, B., Pastor-Galán, D., Degenaar, R., Sadradze, N., Adamia, S., Sahakyan, L., Avagyan, A., Sosson, M. and Rolland, Y., 2017. Progressive orocline formation in the Eastern Pontides–Lesser Caucasus. Geological Society, London, Special Publications, 428(1): 117-143.

Mullender, T.A.T., Frederichs, T., Hilgenfeldt, C., de Groot, L.V., Fabian, K. and Dekkers, M.J., 2016. Automated paleomagnetic and rock magnetic data acquisition with an in-line horizontal “2G” system. Geochemistry, Geophysics, Geosystems, 17(9): 3546-3559.

Nowroozi, A.A., 1972. Focal mechanism of earthquakes in Persia, Turkey, West Pakistan, and Afghanistan and plate tectonics of the Middle East. Bulletin of the Seismological Society of America, 62(3): 823-850.

Ogg, J.G., Ogg, G. and Gradstein, F.M., 2016. A Concise Geologic Time Scale: 2016. Elsevier.

Opdyke, N.D., Johnson, N.M., Johnson, G.D., Lindsay, E.H. and Tahirkheli, R.A.K., 1982. Paleomagnetism Of The Middle Siwalik Formations Of Northern Pakistan And Rotation Of The Salt Range Decollement. Earth, 37: 1-15.

Opdyke, N.D., Lindsay, E., Johnson, N., Tahirkheli, R.A.K. and Mirza, M.A., 1979. Magnetic polarity stratigraphy and vertebrate paleantology of the upper Siwaliksub- Group of northern Pakistan. Palaeogeography,Palaeoclimatology,Palaeoecology, 27: 1-34.

Pastor-Galán, D., Mulchrone, K.F., Koymans, M.R., van Hinsbergen, D.J.J. and Langereis, C.G., 2017. Bootstrapped total least squares orocline test: A robust method to quantify vertical-axis rotation patterns in orogens, with examples from the Cantabrian and Aegean oroclines. Lithosphere, 9(3): 499-511.

Pennock, E.S., Lillie, R.J., Zaman, A.S.H. and Yousaf, M., 1989. Structural interpretation of seismic reflection data from eastern Salt Range and Potwar Plateau, Pakistan. AAPG Bulletin, 73(7): 841-857.

Pilbeam, D., Barry, J., Meyer, G.E., Shah, S.M.I., Pickford, M.H.L., Bishop, W.W., Thomas, H. and Jacobs, L.L., 1977. Geology and palaeontology of Neogene strata of Pakistan. Nature, 270(5639): 684-689.

Powell, C.M. and Conaghan, P.J., 1973. Plate tectonics and the Himalayas. Earth and Planetary Science Letters, 20(1): 1-12.

Sarwar, G. and DeJong, K.A., 1979. Arcs, oroclines, syntaxes: the curvature of mountain belts in Pakistan. Geodynamics of Pakistan: 341-349.

Stanley, S.M., 2005. Earth system history. Macmillan.

Tauxe, L., 2010. Essentials of paleomagnetism. Univ of California Press.

Tauxe, L. and Opdyke, N.D., 1982. A Time Framework Based On Magnetostratigraphy For The Siwalik Sediments Of The Khaur Area, Northern Pakistan. Paleogeography, Palaeoelimatology, Palaeoecology, 37: 43-61.

Torsvik, T.H., Van der Voo, R., Preeden, U., Mac Niocaill, C., Steinberger, B., Doubrovine, P.V., van Hinsbergen, D.J.J., Domeier, M., Gaina, C., Tohver, E., Meert, J.G., McCausland, P.J.A. and Cocks, L.R.M., 2012. Phanerozoic polar wander, palaeogeography and dynamics. Earth-Science Reviews, 114(3): 325-368.

Van Hinsbergen, D.J.J., Lippert, P.C., Dupont-Nivet, G., McQuarrie, N., Doubrovine, P.V., Spakman, W. and Torsvik, T.H., 2012. Greater India Basin hypothesis and a two-stage Cenozoic collision between India and Asia. Proceedings of the National Academy of Sciences, 109(20): 7659-7664.

van Velzen, A.J. and Zijderveld, J.D.A., 1995. Effects of weathering on single-domain magnetite in Early Pliocene marine marls. Geophysical Journal International, 121(1): 267-278.

Warwick, B.P.D., 1993. Overview of the Geography , Geology , and Structure of the Potwar Regional Framework Assessment Project Study. U.S. Geological Survey, Bulletin 2078-A: -.

Wensink, H., 1972. The Paleomagnetism of the salt pseudomorph beds of middle Cambrian age from the Salt Range, West Pakistan. Earth and planetary science letters, 16(2): 189-194.

Yeats, R.S., Khan, S.H. and Akhtar, M., 1984. Late Quaternary deformation of the Salt Range of Pakistan. GSA Bulletin, 95(8): 958-966.

Yeats, R.S. and Lillie, R.J., 1991. Contemporary tectonics of the Himalayan frontal fault system: folds, blind thrusts and the 1905 Kangra earthquake. Journal of Structural Geology, 13(2): 215-225.

Zijderveld, J.D.A., 1967. AC demagnetization of rocks: analysis of results, Developments in solid earth geophysics. Elsevier, pp. 254-286.